STATE RESEARCH CENTER OF RUSSIA

INSTITUTE FOR HIGH ENERGY PHYSICS

IHEP 96-52



V.Ammosov, V.Korablev*), V.Zaets

# ELECTRIC FIELD AND CURRENTS IN RESISTIVE PLATE CHAMBER

Submitted to *NIM*

*)Correspondent author. E–mail: korablev@mx.ihep.su

Protvino 1996

UDK 537.613

M–24


## Abstract

Ammosov V., Korablev V., Zaets V. Electric Field and Currents in Resistive Plate Chamber: IHEP Preprint 96-52. – Protvino, 1996. – p. 18, figs. 11, refs.: 3.

A method of three–dimensional electric fields calculation that takes into account the presence of surface currents has been realized. Different versions of the resistive plate chamber (RPC) design were simulated. Calculations of electric fields, currents and comparison with the measured values of currents were made. Recommendations relative to an optimal graphite coating in the basic RPC scheme under consideration are given.



## Аннотация

Аммосов В., Кораблев В., Заец В. Электрическое поле и токи в резистивной плоскопараллельной камере: Препринт ИФВЭ 96-52. – Протвино, 1996. – 18 с., 11 рис., библиогр.: 3.

Реализован метод вычисления трехмерных электрических полей, учитывающий присутствие поверхностных токов. Произведено моделирование различных вариантов резистивной плоскопараллельной камеры (РПК). Выполнен расчет электрических полей, токов и сделано сравнение с измеренными значениями токов. Выработаны рекомендации относительно оптимального графитового покрытия для основной рассматриваемой схемы РПК.

## Introduction

Knowledge of calculated electric fields and currents allows one to understand the processes that occur in a device under the high voltage supplied and to provide concrete recomendations relative to the design and materials to be used.

There arise two types of surface charges when the voltage is supplied to a medium boundary: induced charge due to the dielectric molecules polarization in the external field and free charge due to the volume current passage through a boundary. Procedures for electric field calculation in electrostatic and current approaches are available [1]. But physics publications with recommendations how to take into account the presence of the surface currents that can be even above the volume currents are lacking.

This paper shows a possibility to involve surface currents in the procedure of electric field calculation using the law of full current conservation.

Because of the analogy between electric and magnetic field description, ideology and mathematical formalizm for electric field calculation are taken from [2]. The magnetic field [2] is presented as superposition of fields from conductor and surface (from magnetized iron) currents. A surface charges method (SCM) proposed describes the electric field as superposition of fields from surface charges. Both methods use boundary conditions for field penetration: conservation of tangential strength and normal magnetic induction (electric shift). In [2] an absolute field scale and the flux distribution in the iron are defined by the law of full current conservation (circulation of strength vector around the conductor). In SCM a field scale and the flux distribution in the medium are also defined by strengh circulation along unclosed trajectory (potential losses either between electrodes or electrode and surface with the ground potential).

## 1. General considerations

Let the electric field penetrate through the small horizontal surface element $ds=(dt)^2$ from the lower ($E_1$) to upper ($E_2$) medium and surface current flows along tangential

(surface) field component $E_t$ from the left ($E_{tl}$, $I_{tl}$) to the right ($E_{tr}$, $I_{tr}$) side of the element. Let $\varphi$ be the angle between field and its normal component $E_n$.

The two first equations for the electric field calculation are the well-known ones for the tangential and normal strength passage through boundary:

$$E_{2t} - E_{1t} = 0, \tag{1}$$

$$\varepsilon_2 \cdot E_{2n} - \varepsilon_1 \cdot E_{1n} = \sigma_f \tag{2}$$

$\varepsilon$ is permittivity, $\sigma_f$ is surface free charge density.

Here and later on the formulas are written in the system Volt, Ampere, Coulomb, metre, second and surface charge density is defined as $\sigma=(1/\varepsilon_0)(dQ/dS)$. Factor $1/4\pi$ is marked as "k".

For the current flow through a small surface element we require the incoming current to be equal to the outcoming one:

$$dI_{tl} + dI_{1v} = dI_{tr} + dI_{2v}, \tag{3}$$

here $dI_{tl}$ is the surface current incoming from the left side, $dI_{1v}$ is the volume current incoming from the lower volume part, $dI_{tr}$ is the surface current outcoming in the right side and $dI_{2v}$ is the volume current outcoming in the upper volume part.

Substitute surface ($dI_t$) and volume ($dI_v$) currents by their equivalent expressions through strengths and resistivities:

$$dI_t = \frac{E_t}{R} dt, \tag{4}$$

$$dI_v = \frac{E \cdot (ds \cdot cos\varphi)}{\rho} = \frac{E_n}{\rho} ds, \tag{5}$$

here $\rho$ is the volume resistivity ($\Omega$·cm), R is the surface resistivity ($\Omega/\square$).

Then eq.(3) can be rewritten as:

$$(\frac{E_{2n}}{\rho_2} - \frac{E_{1n}}{\rho_1})ds = -\frac{E_{tr} - E_{tl}}{R} dt. \tag{6}$$

After dividing both parts of eq.(6) by $ds=(dt)^2$ the final equation for the law of full current conservation looks like:

$$\frac{E_{2n}}{\rho_2} - \frac{E_{1n}}{\rho_1} = -\frac{dE_t}{dt}\frac{1}{R}. \tag{7}$$

Thus, the surface current is involved in the law of full current conservation as a gradient of the tangential field $dE_t/dt$ along its direction. So, the jump of the volume current at the boundary is due to the presence of tangential field gradient along the surface.

Other possible expressions for the right part of eq.(7) are:

$$\frac{dE_t}{dt}\frac{1}{R} = \frac{d\sigma_f}{dt} \cdot |v| = \frac{|E_t|}{|\sigma_f|}\frac{d\sigma_f}{dt}\frac{1}{R}. \tag{8}$$

Here $d\sigma_f/dt$ is the gradient of surface free charge density along $E_t$ direction, $|v|$ is the absolute value of free charge velocity.

As a rule in electric field tasks eq.(7) is applied with the zero right part, but near the sharp corners the tangential field gradient is by two or three orders higher, than the absolute field value, and the correct solution requires that the volume current jump due to the tangential field gradient be taken into account.

A field scale and the flux distribution in medium are given by the potential losses equation:

$$\int_{\ell}(\vec{E}\cdot\vec{d\ell}) = \Delta U, \tag{9}$$

or by equivalent to it equation for surface potential:

$$U = k\cdot\int_{s}\frac{\sigma(r)}{r}ds, \tag{9'}$$

here $r$ is the radius from the surface point to a point of potential definition.

Under the vacuum consideration the electric field on opposite sides of the small surface element can be expressed as:

$$E_2 = E_{ex} + E_{own}, \tag{10}$$

$$E_1 = E_{ex} - E_{own} \tag{11}$$

here $E_{ex}$ is the external field created by all surface charges excluding the given element, $E_{own}$ is the own field created by surface charge of the given element. Then eqs.(1), (2) and (7) can be transformed respectively to the following form:

$$2\cdot E_{own_t} = 0, \tag{12}$$

$$(\varepsilon_2+\varepsilon_1)\cdot E_{ex_n} + (\varepsilon_2-\varepsilon_1)\cdot E_{own_n} = \sigma_f, \tag{13}$$

$$(\frac{1}{\rho_2}+\frac{1}{\rho_1})\cdot E_{ex_n} + (\frac{1}{\rho_2}-\frac{1}{\rho_1})\cdot E_{own_n} = -\frac{dE_t}{dt}\frac{1}{R}. \tag{14}$$

Eq.(12) is automatically satisfied because its tangential field in the central point of elementary square is equal to zero (see Appendix).

Thus, if we work in terms of $E_{ex}$, $E_{own}$ the system of eqs.(1), (2), (7) is equivalent to the system of eqs.(13), (14).

Now, if we divide the surface into a large amount of small elements and assume the surface charge density $\sigma$ to be a constant value in the internal region of every element, the electric field in any space point can be expressed as:

$$\vec{E} = k\cdot\sum_{j}\sigma_j A_j\int_{s_j}\frac{\vec{r}}{r^3}ds, \tag{15}$$

here $A_j$ is the transformation (3×3) matrix from "j" element to space, $\vec{r}$ is the radius–vector from "j" element to a space point in the intrinsic frame of reference of "j" element.

Let $\vec{G}$ denote the 3–dimensional vector–integral (see Appendix)

$$\vec{G}_j = k \cdot \int_{s_j} \frac{\vec{r}}{r^3} ds \tag{16}$$

and $\vec{n}$ be the normal vector to the surface element, then eqs.(13) and (14) for every "i" surface element can be written as:

$$(\varepsilon_2 + \varepsilon_1) \cdot \sum_{j \neq i} \sigma_j \cdot ((A_j \vec{G}_j) \cdot \vec{n}_i) + (\varepsilon_2 - \varepsilon_1) \cdot \sigma_i \cdot (\vec{G}_i \cdot \vec{n}_i) = \sigma_{f(i)} \tag{17}$$

$$(\frac{1}{\rho_2} + \frac{1}{\rho_1}) \cdot \sum_{j \neq i} \sigma_j \cdot ((A_j \vec{G}_j) \cdot \vec{n}_i) + (\frac{1}{\rho_2} - \frac{1}{\rho_1}) \cdot \sigma_i \cdot (\vec{G}_i \cdot \vec{n}_i) = -\frac{dE_{t(i)}}{dt} \frac{1}{R} \tag{18}$$

and eq.(9) for the potential losses along contour $\ell_i$ that starts from "i" element and is divided into "m" segments $\Delta \vec{\ell}_{im}$ is now:

$$\sum_m ((\sum_j \sigma_j A_{jm} \vec{G}_{jm}) \cdot \Delta \vec{\ell}_{im}) = \Delta U_i. \tag{19}$$

Eq.(9') for the potential in the centre of "i" element from all surface charges:

$$U_i = k \cdot \sum_j \sigma_j \cdot \int_{s_j} \frac{ds}{r}. \tag{19'}$$

Later on, when we say eq.(19), it means either eq.(19) or eq.(19').

When volume and surface currents are flowing, for the dielectric surface we use eqs.(17) and (18). Graphite and strip planes are connected with high–voltage source and the ground with the known potentials, therefore for them we use eqs.(17) and (19) for surface elements of the direct voltage and ground supplying and eqs.(17) and (18) for all other elements. But when graphite and strip resistivities are neglegible in comparison with neighbour plastic resistivities we can suppose that graphite and strip planes are the surfaces of the constant potential and use for all their elements eqs.(17) and (19).

Thus, for the RPC surface divided into "N" elements we have the set of "2N" linear equations with "2N" unknowns. Each surface element contains two unknowns: $\sigma$ is the total charge density and $\sigma_f$ is the free charge density. Induced charge density is defined, hence, as $\sigma_{ind} = \sigma - \sigma_f$.

When only volume current is allowed to flow, we use the same set of equations as above, but eq.(18) applies with the zero right part which is equivalent to infinite value of surface resistivity R (surface current doesn't flow).

In case of electrostatic approach for the dielectric surface we use only eq.(17) with zero right part. The current doesn't flow and this surface has no free charges and $\sigma = \sigma_{ind}$.

For surfaces connected with "infinite" sources of free charges (high–voltage source and the ground) we use eq.(17) with nonzero right part and eq.(19). High–voltage source initiates the potential difference with free charges and the ground provides the zero potential with free charges as well. And in elecrostatic task with "M" dielectric surface elements and "N" conductor surface elements we have M + 2N equations and M + 2N unknowns.

In electrostatic and volume current approaches we get a set of unknowns directly from the solution of the system of linear equations. But when we include surface currents the procedure of solution is now the iteration procedure.

At the first step we solve the system of linear equations with zero right part of eq.(18). Then we include iteration fit procedure: define numerical values of tangential strengths derivatives $dE_t/dt$ for each dielectric surface element and repeat calculation with nonzero right part of eq.(18), redefine new values of derivatives and so on up to fit procedure convergence. When fluctuations of unknowns from iteration to iteration are neglegible in comparison with the absolute values of unknowns we stop iteration procedure.

In Appendix it is shown, that strength derivative $dE_t/dt$ can be presented as a linear combination of unknowns $\sigma$. In this case we recalculate not derivatives $dE_t/dt$, but tangential field directions $\vec{t}$, that practically don't change from iteration to iteration and fit procedure converges more quickly.

Sometimes (nonsymmetry field, complex device configuration and a lot of sharp corners) we have no possibility (because of the restricted computer memory) to divide the surface into a sufficient amount of small elements to take into account correctly the field behaviour near the corners. Experience has shown, that in this case the substitution of derivative $dE_t/dt$ by free charge density with coefficient $\lambda \cdot \sigma_f$, where coefficient $\lambda$ is about $0.05 \div 0.1$, is very effective. This substitution allows one: a) to divide the surface into the smaller number of big elements and the result is practically the same as for the correct solution ($dE_t/dt$ with the large amount of small surface elements), b) the system of linear equations is solved directly without iteration procedure. Thus, we gain advantage in computer memory and time without loss in solution accuracy.

## 2. Field and currents in RPC

The basic scheme of Resistive Plate Chamber (RPC) is shown in Fig.1. Insulation film: volume resistivity $\rho = 5 \cdot 10^{15}$ $\Omega$·cm, surface resistivity $R = 5 \cdot 10^{15}$ $\Omega/\square$, permittivity $\varepsilon = 3$. Bakelite(phenolic polymer): $\rho = 10^{12}$ $\Omega$·cm, $R = 10^{12}$ $\Omega/\square$, $\varepsilon = 4$. Spacers and frame(polyvinil chloride — PVC): $\rho = 5 \cdot 10^{15}$ $\Omega$·cm, $R = 5 \cdot 10^{15}$ $\Omega/\square$, $\varepsilon = 3$. Gas: $\rho = 10^{18}$ $\Omega$·cm, $\varepsilon = 1$.

The supplied voltage between graphite electrodes is 8 kV. The field has the down direction. Both strip planes (each strip–line through 50 $\Omega$ resistance) and lower graphite electrode are shunted on the ground. Thus, the voltage between the upper graphite electrode and strip plane is 8 kV, but the lower graphite electrode and strip plane have practically the same (ground) potential.

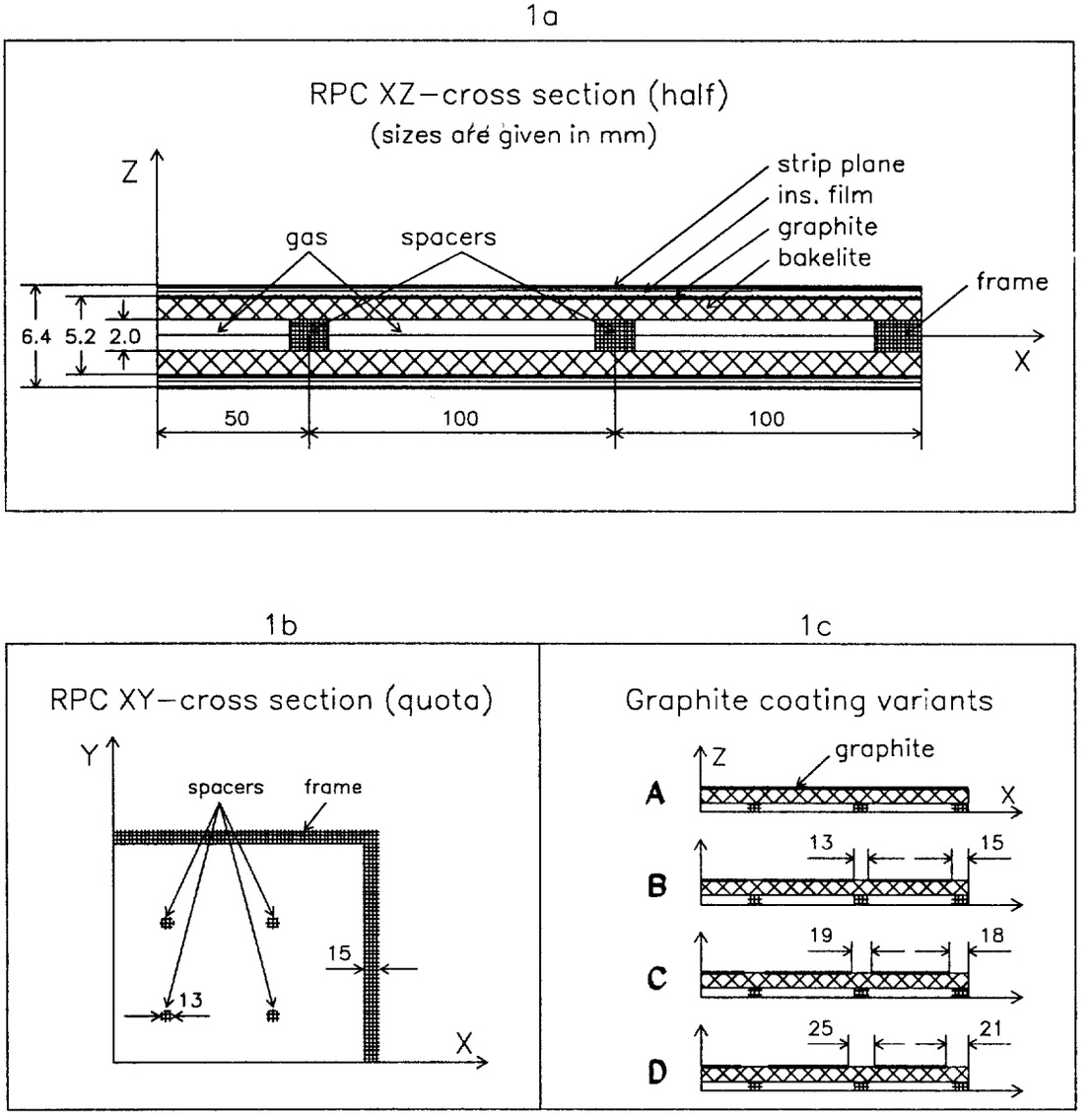


Fig. 1. RPC scheme and graphite coating.

Graphite surface resistivity R=$10^5$ $\Omega/\Box$ is very small in comparison with bakelite resistivity. Strip (copper foil) resistivity is also neglegible relative to insulation film resistivity. We suppose that graphite and strip planes are the surfaces of constant potential and in calculations for them we apply eqs.(17) and (19) which don't contain resistivities.

The questions desirable to be resolved by calculating the electric field in RPC are:

a) qualitative understanding of field behaviour;
b) indicating of regions with high local field strength;
c) estimation of current leakage;
d) field and current dependence on graphite coating.

For these purposes we simulated 4 variants of graphite coating (see Fig.1c). Variant A — the whole plane is covered with graphite, variant B — the surface opposite to the spacers and the frame is not covered with graphite, variant C — variant B plus 3 mm zone around the spacers and along the frame is not covered with graphite, variant D — variant B plus 6 mm zone around the spacers and along the frame is not covered.

Electric field calculation depends on the used approach. Average strengths in the sensitive gas, bakelite, spacers and frame for variant A of graphite coating and for different approaches are given in Table 1. Strengths are presented as (E/4kV/mm)×100%.

**Table 1.** Strengths for variant A of graphite coating.

| | approach | $E_{gas}$ | $E_{bak.}$ | $E_{spac.}$ | $E_{fram.}$ |
|---|---|---|---|---|---|
| 1 | electrostatic | 71.43 | 17.85 | 47.95 | 45.40 |
| 2 | volume currents | 100.00 | 0.00 | 99.99 | 98.94 |
| 3 | volume + surface currents | 99.84 | 0.09 | 99.54 | 98.47 |

These data show, that in electostatic solution only 71.43% of maximum possible strength is realized in the sensitive gas. When the volume current is allowed to flow, the supplied voltage is concentrated in high resistivity (relative to bakelite) materials: gas, spacers, frame. Additional channel for surface currents in variant A of graphite coating slightly redistributes strengths in materials.

The role of the surface currents is noticeable if we compare strengths in the spacers and the frame, for example, in variant B of graphite coating (Table 2).

**Table 2.** Strengths for variant B of graphite coating.

| | approach | $E_{gas}$ | $E_{bak.}$ | $E_{spac.}$ | $E_{fram.}$ |
|---|---|---|---|---|---|
| 1 | electrostatic | 71.43 | 17.85 | 10.91 | 2.62 |
| 2 | volume currents | 100.00 | 0.00 | 98.52 | 77.22 |
| 3 | volume + surface currents | 99.84 | 0.09 | 69.37 | 33.81 |

In variants C and D of graphite coating the influence of the surface currents on strength distribution in the spacers and the frame is more pronounced.

Figs.2÷10 show the results for the RPC scheme with strip planes.

The electric field behaviour in the spacer region for different variants of graphite coating is shown in Fig.2. In variant A the field has mostly the vertical orientation. For the broken coatings (variants B,C,D) in bakelite significant horizontal components arise and the field from the graphite end is splitted into two fluxes. One flux is directed to the upper strip plane, the other through the spacer in the down direction. Qualitatively the same picture is observed in the frame region (Fig.3). Such field behaviour attests that there can arise significant tangential field components near the spacer and frame corners.

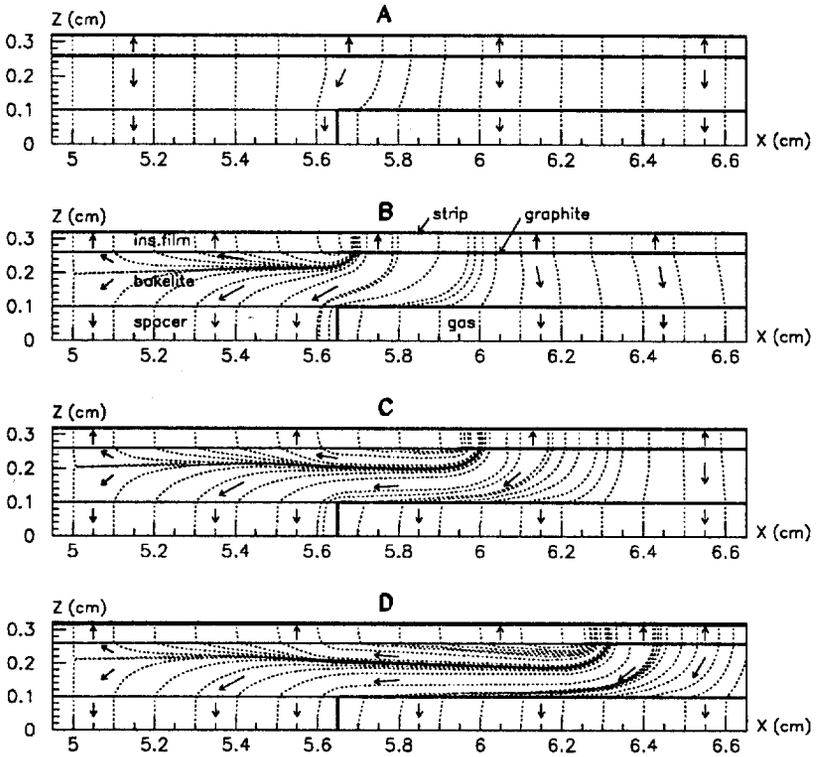


Fig. 2. Field behaviour in the spacer region.

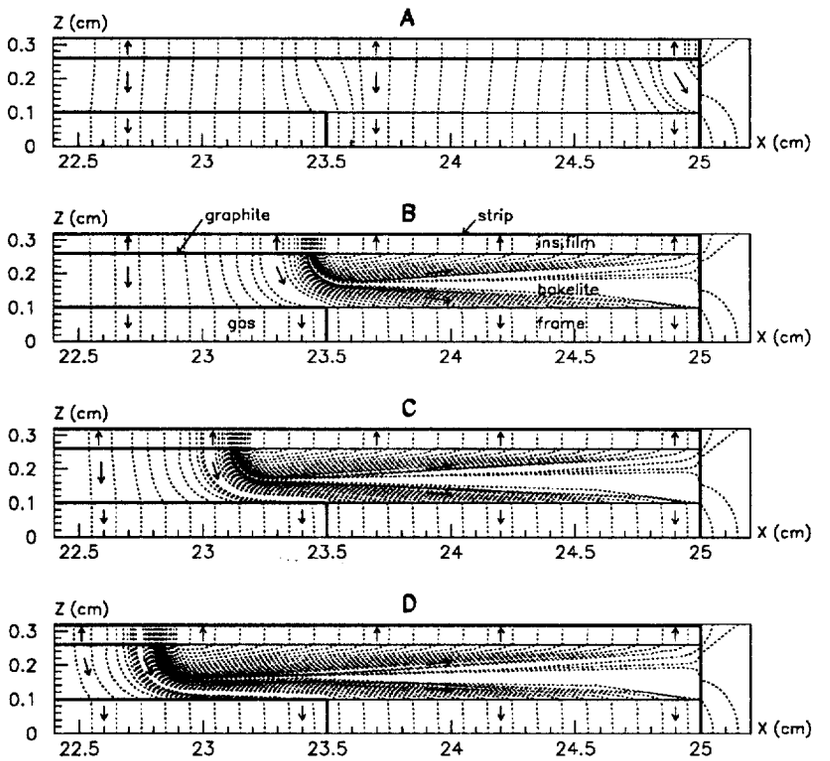


Fig. 3. Field behaviour in the frame region.

Fig.4 shows the vertical $E_z$ dependence on X coordinate when we are moving from the RPC centre to the peripheral zone and cross the spacers and the frame in the central (Z=0) plane. The value of the field is normalized on 4 kV/mm. For variant A the field is practically a plato (99% from 4 kV/mm) in the bulk of the RPC region. Variant B gives the significant field falling in the spacers and the frame in comparison with variant A (approximately by a factor of 2) and then (variants C and D) the falling becomes weaker. From variant B to D in the gas near the spacers and the frame there arises and grows the region with the field less than the plato.

When we are moving along the bakelite–gas boundary from the gas side (Fig.5) $E_z$ field behaviour qualitatively repeats $E_z$ behaviour in the central (Z=0) plane, which testifies to the weak $E_z$ dependence on Z–coordinate in the sensitive gas.

Along the bakelite–gas boundary there arise significant tangential field components near the corners (Fig.6). For variant A a very large tangential field (of the same order as vertical) appears near the external frame corner. Variant B shows approximately 50% (from plato) tangential field near the spacers and internal frame corners. And then — variants C and D — the tangential field near the corners is falling.

The absolute value of the field along the bakelite–gas boundary at Z=0.099cm is shown in Fig.7. Variant A gives the field near the external frame corner even above the plato — about 5 kV/mm (extreme field in the frame corner is 8.4 kV/mm). High strength $\sim$ 24 kV/mm is concentrated at the very end of the graphite coating. These local high strengths in the region of plastic — atmosphere boundary don't exclude (in the case of variant A) a spark arising along the external lateral RPC surface. At a distance of 1mm in the X–direction from the graphite end and the frame corner the field quickly falls down to value $\sim$ 2 kV/mm both near the frame corner and the graphite end.

The integral form of eqs.(4) and (5) was applied for the surface and volume currents calculation. Tables 3 and 4 give the detailed information about the volume and surface currents flowing through the spacers, frame, insulation film and gas in the given RPC scheme for two modifications: left–hand (relative to symbol "/") values are the currents for the scheme with strip planes, right–hand ones — for the scheme without strips. For the spacers the current is summerized over 16 spacers.

**Table 3.** Volume currents(nA) in RPC.

| | A | B | C | D |
|---|---|---|---|---|
| spacers | 0.22 / 0.22 | 0.15 / 0.20 | 0.08 / 0.20 | 0.05 / 0.19 |
| frame | 2.29 / 2.29 | 0.78 / 1.45 | 0.46 / 1.15 | 0.31 / 0.95 |
| ins.film | 66.63 / - | 61.21 / - | 59.92 / - | 59.35 / - |
| gas | 0.09 / 0.09 | 0.09 / 0.09 | 0.09 / 0.09 | 0.09 / 0.09 |

**Table 4.** Surface currents(nA) in RPC.

| | A | B | C | D |
|---|---|---|---|---|
| spacers | 0.66 / 0.66 | 0.55 / 0.64 | 0.34 / 0.63 | 0.23 / 0.61 |
| frame | 2.72 / 2.73 | 1.26 / 1.85 | 0.76 / 1.47 | 0.51 / 1.21 |
| ins.film | 3.19 / - | 0.62 / - | 0.33 / - | 0.18 / - |

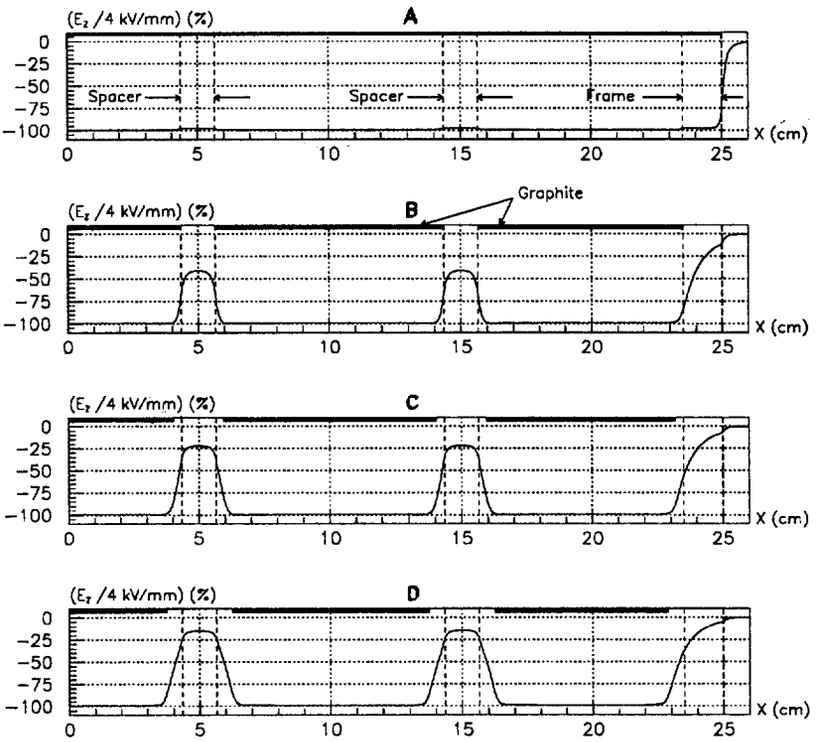


Fig. 4. Vertical $E_z$ dependence on X coordinate at Y=5 cm, Z=0.

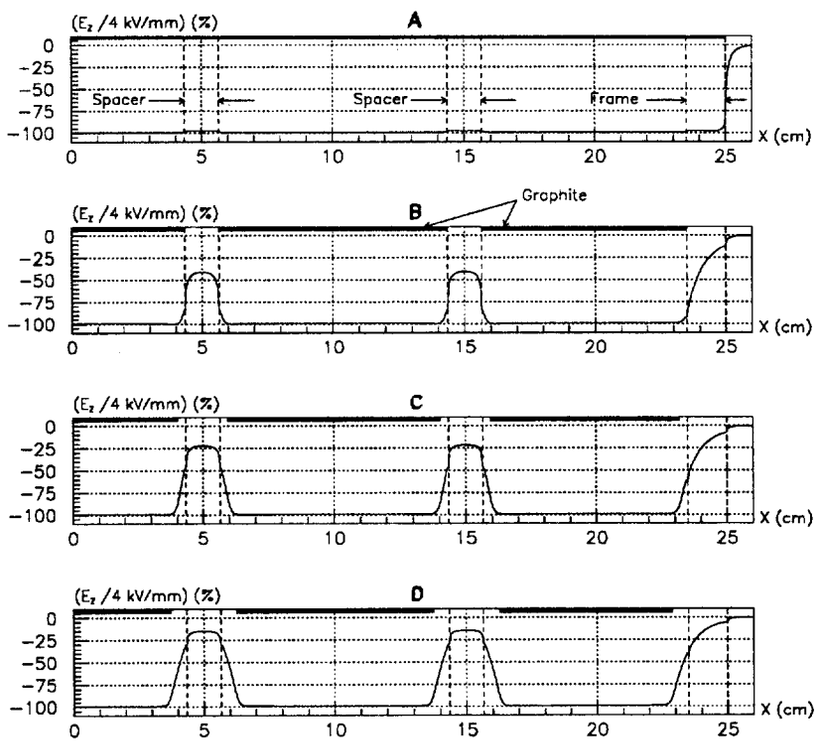


Fig. 5. Vertical $E_z$ field dependence on X coordinate at Y=5 cm, Z=0.099 cm.

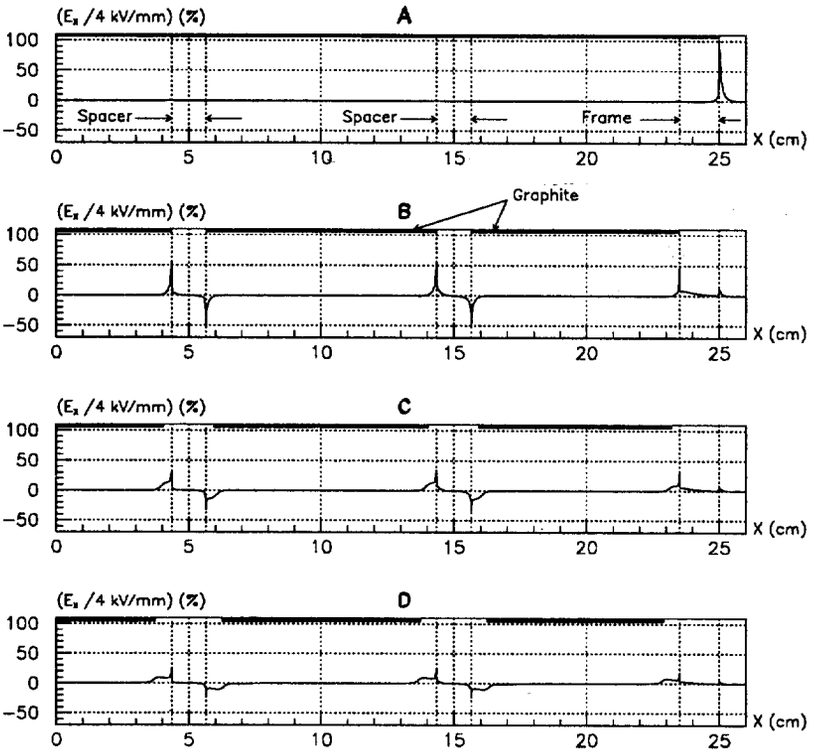


Fig. 6. Tangential $E_x$ field dependence on X coordinate at Y=5 cm, Z=0.099 cm.

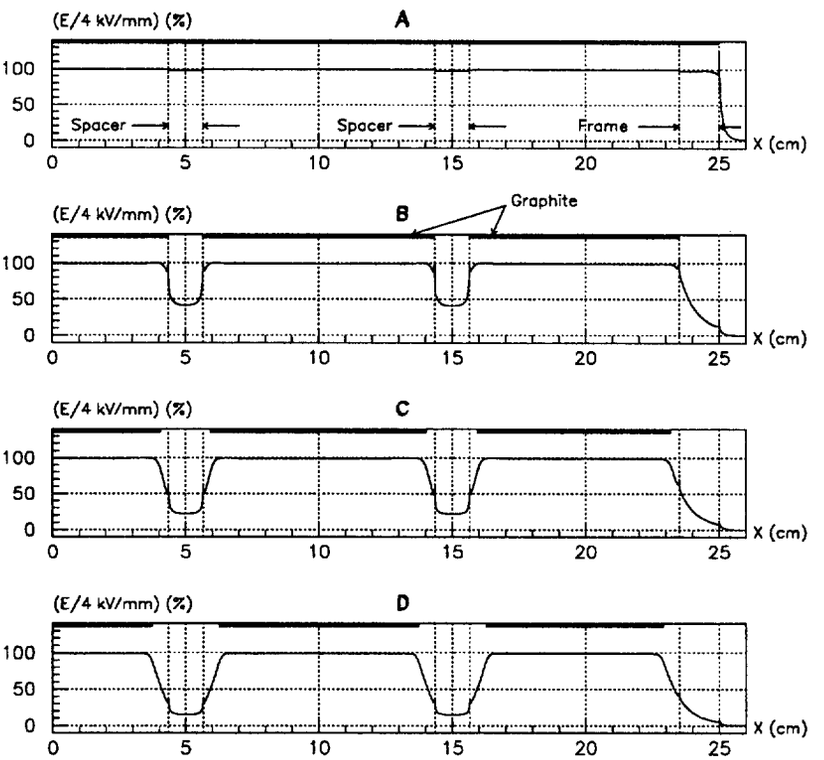


Fig. 7. $/E/$ dependence on X coordinate at Y=5 cm, Z=0.099 cm.

Graphically for the RPC scheme with strips the dependence of the current leakage through the spacers and frame on graphite coating is shown in Fig.8. As an argument we have used the width of zone that is not covered with graphite in the region of frame. The value of surface current exceeds the volume current by $\sim 1/3$ for variant A and by a factor of $\sim 2$ for B, C and D. The total current leakage through the spacers and the frame falls with the extension of an uncovered region 5 times (from 5.9 nA down to 1.1 nA).

Different situation we have with the current flowing through the insulation film (see Table 3 and 4). Here the total current has the weaker dependence on the graphite coating and falls from 70 nA (variant A) down to 60 nA (variant D).

It is necessary to note that the current, flowing through the spacers and the frame in the scheme without strip planes, falls from 5.9 nA (variant A) down to 3 nA (variant D) that is by a factor of 2 against factor 5, when strips are present. Increase of the current is due to the redistribution of electric field in the region of the spacers and the frame. The flux in bakelite in Fig.2 and 3 (variants B,C,D) that was oriented to strip plane in the upper direction, now in variant without strips is flowing in the lower direction and the strength in the spacers and the frame increases.

For the current leakage through the insulation film to be compatible with the current through spacers and frame (to reduce the total current leakage) it is necessary to increase the insulation film resistivity and thickness.

Negative circumstance arises (Fig.9) with the variation of graphite coating — nonhomogeneous field region in the sensitive gas around the spacers and along the frame grows from variant A to D. The square of gas region with nonhomogeneous field normalized over the total RPC square is extending from 0.4% (variant B) up to 5% (variant D) and is defined mostly by the nonhomogeneous gas region along the frame.

Graphite free charge density distribution for the upper electrode is shown in Fig.10. Practically, this distribution is the plato excluding graphite ends — narrow strips around the spacers and along the frame with higher charge concentration. The lower electrode shunted on the ground has the surface charge density by an order of 4 lower.

The average free and induced surface charge densities (in $\mu C/m^2$) for different planes (boundaries) are given in Table 5. Coordinate Z=$\pm$3.2 mm is for the upper and lower strip planes respectively, Z=$\pm$2.6 mm — for the graphite planes, Z=$\pm$1.0 mm — for the upper and lower bakelite–gas boundaries.

**Table 5.** Average surface charge densities.

| Z (mm) | 3.2 | 2.6 | 1.0 | −1.0 | −2.6 | −3.2 |
|---|---|---|---|---|---|---|
| $\sigma_{free}$ ($\mu C/m^2$) | −354.1 | 354.1 | 35.2 | −35.2 | 0.3 | −0.4 |
| $\sigma_{ind.}$ ($\mu C/m^2$) | 236.1 | −236.1 | 0.1 | −0.1 | −0.2 | 0.3 |
| $\sigma_{tot.}$ ($\mu C/m^2$) | −118.0 | 118.0 | 35.3 | −35.3 | 0.1 | −0.1 |

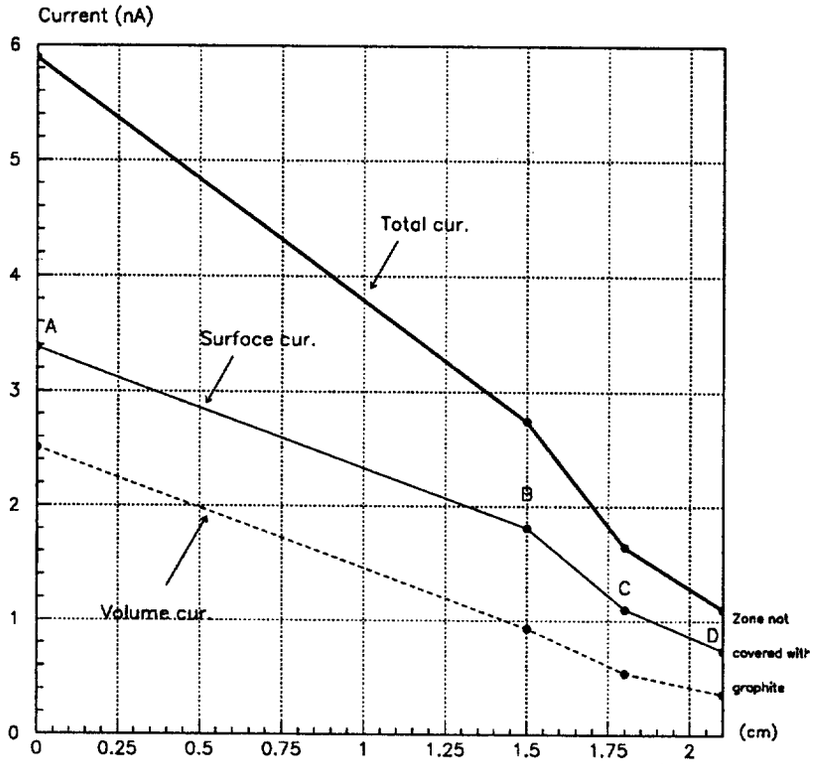


Fig. 8. Current leakage through spacers and frame.

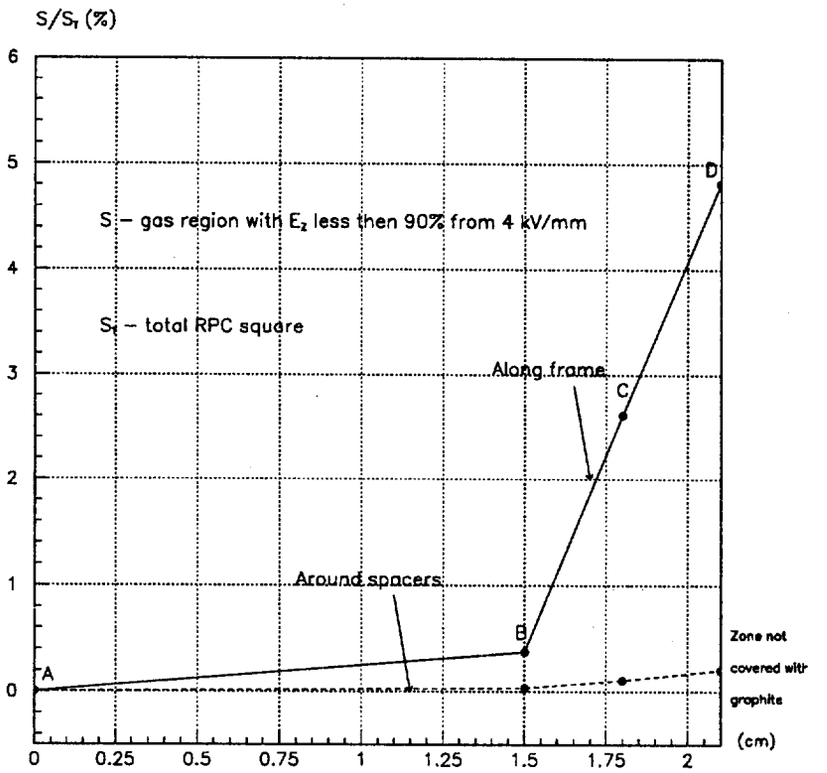


Fig. 9. Value of nonhomogeneous field region.

The strength estimation between two planes with equal but opposite sign charges in contrast to a purely electrostatic task, when we use formula $E = \sigma_{tot}/\epsilon$, now that the current is allowed to flow is somewhat different $E = \sigma_{free}/(\epsilon_2 - \epsilon_1(\rho_1/\rho_2))$. Here $\epsilon_2$, $\rho_2$ are the internal (relative to planes) medium permittivity and resistivity, $\epsilon_1$, $\rho_1$ are for the external medium and $\sigma_{free}$ is the surface free charge density on the boundary of internal and external mediums. This estimation follows from eqs.(2) and (7) with the zero right-hand part of eq.(7) — surface current doesn't flow.

The choice of the optimal graphite coating was based on the following requirements: maximum homogeneity of the field in the gas region (field not less than 90% of 4 kV/mm), minimum current leakage through RPC materials, the absence of the zones with high local strength. From this point of view for the RPC configuration including the strip planes, when the value of the current has the weak dependence on the graphite coating, variant A of graphite coating for the spacers and variant C for the frame provide the maximum homogeneous field (nonhomogeneous region in the gas is no more than 3% from the RPC square) and exclude the high field strength near the spacers and frame corners. For the RPC configuration without strip planes variant C for the spacers and the frame allows one, on the one hand, to have the homogeneous field in the gas (nonhomogeneity is also about 3%) and, on the other hand, to decrease the current leakage relative to variant A approximatelly two times.

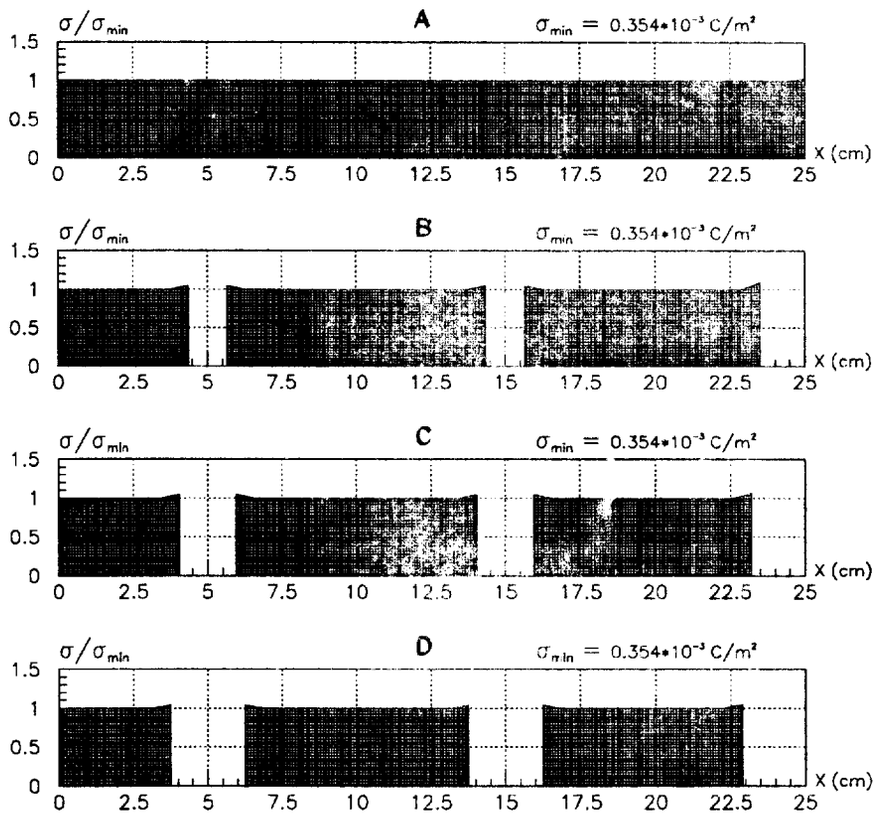


Fig. 10. Graphite free charge density distribution.

## 3. Comparison of measured and calculated currents

The capabilities of the proposed electric fields calculation procedure (SCM) were verified by the direct comparison between the measured and calculated currents for different RPC compositions (Fig.11). The measured current is marked by black points, the solid line represents the calculation by the SCM method and the broken line is the estimation by the Ohm law I=U/$R_{eff}$ ($R_{eff}$ is the effective RPC scheme resistance). Surface and volume resistances of RPC elements with the same Z–coordinate are included for the effective resistance calculation in parallel. The assumption for the Ohm law estimate was made: each global Z–plane that separates one set of RPC elements from the other is the equipotential plane.

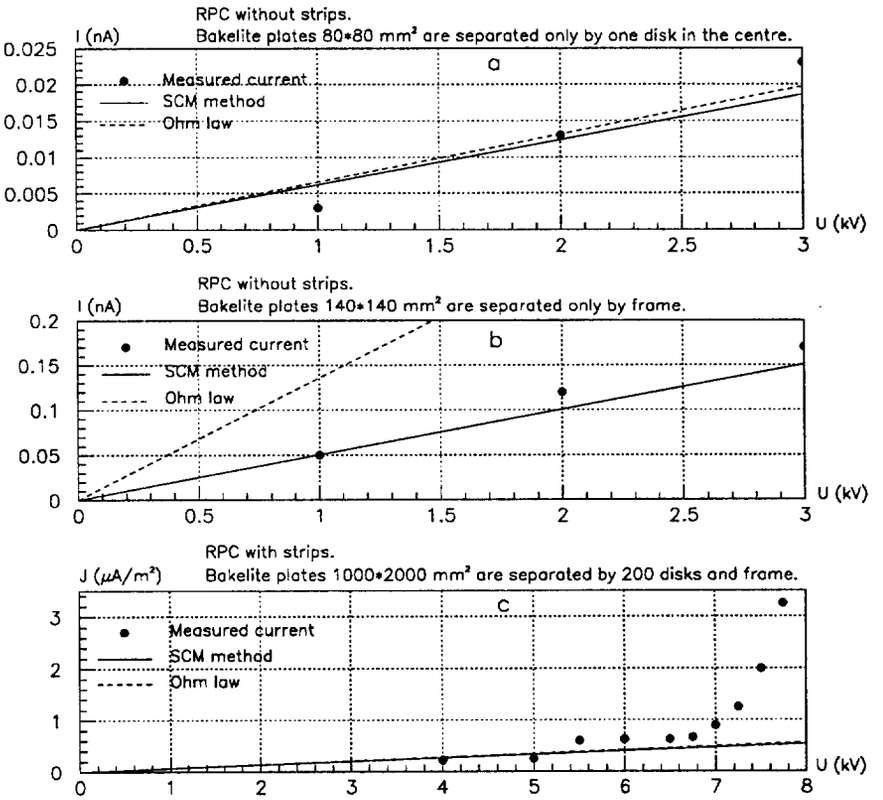


Fig. 11. Measured and calculated currents in different RPCs.

Some of measurements (Fig.11a,b) were performed by us. The data for the high resistivity RPC of another group [3] are shown in Fig.11c. The materials for the RPCs were practically of the same order of resistivity.

In calculations we haven't changed resistivity and permittivity with the voltage supplied, therefore have the linear current–voltage dependence. In practice the material characteristics (especially gas resistivity) vary at very high voltage. Thus, it is reasonable to compare the measured and calculated currents only in the region of not so high voltage – the region of linear current–voltage behaviour.

Fig.11a shows the measured and calculated currents for the following RPC composition: bakelite plates 80×80 mm$^2$, graphite 70×70 mm$^2$, bakelite plates are separated by the single 12 mm diameter spacer in the centre. The zone of 20 mm in diameter above and lower the spacer has no graphite coating. Strip planes are absent.

Fig.11b presents the current comparison for the following RPC scheme: bakelite plates 140×140 mm$^2$ are separated only by the frame 5 mm wide, graphite 100×100 mm$^2$, strip planes are absent.

Both these plots give satisfactory agreement of the measured and calculated currents by the SCM method. The Ohm law prediction has large deviation from the measured values in Fig.11b. This deviation points to the fact that in the given variant of the RPC configuration and graphite coating the potential of noncovered (peripheral) surface is significantly less than the potential of the surface with graphite coating.

Fig.11c shows the data for the high resistivity RPC with strip planes [3]. The insulation film thickness here is 0.3 mm. The bakelite plate is 1000×2000×2 mm$^3$. 200 disks of 12 mm in diameter are located at a distance of 100 mm from one another. The graphite coating and frame width are not given in [3]. For definiteness in calculation we used a frame 12 mm wide and variant B for graphite coating (the square against the spacers and the frame is not covered with graphite).

This plot gives satisfactory agreement between the calculated and measured currents in the region of linear current–voltage behaviour and shows that in the RPC with strip planes, when the bulk of the current is defined by the volume current flowing through the insulation film, the Ohm law is capable of the current predicting.

The current leakage through the spacers and the frame relative to the total current leakage for high resistivity RPC [3] is about 2%.

## Conclusion

1. The results given in Sections 2 and 3 show that the realized SCM method is capable of predicting the electric fields and allows one to get both the qualitative understanding of the field picture and the quantitative estimations of the strengths and currents. The calculated currents are in agreement with the measured values in the region of linear current–voltage behaviour for different RPC compositions.

2. The Ohm law is capable of the current predicting for RPC compositions with graphite coating that is close to the unbroken one and can be used as the upper limit for current leakage estimation.

3. In the RPC there exist regions — near spacers and frame corners and graphite coating ends – with the high local strengths.

4. For the RPC scheme under consideration:

4.1. In configuration with strip planes the current leakage practically doesn't depend on the considered graphite coating variants and is mostly defined by the current through the insulation film $\sim 70 \div 60$ nA. The current through the spacers and the frame is $\sim 6 \div 1$ nA.

4.2. In configuration without strips the current leakage is significantly less and decreases by half from 6 nA (variant A) down to 3 nA (variant D).

4.3. In the RPC with strips for the current leakage through insulation film to be compatible with the current leakage through spacers and frame it is desirable to increase the resistance of insulation film at least by an order of magnitude.

4.4. The surface current through the spacers and the frame is systematically above the volume current.

4.5. The requirement of the maximum field homogeneity in the sensitive gas, minimum current leakage and the absence of the zones with the high local strength can be satisfied: in case of the RPC configuration with strip planes as variant A of graphite coating for the spacers and variant C for the frame; for the RPC configuration without strip planes as variant C. Nonhomogeneous gas region for both the RPC configurations is about 3% of the total RPC square.

## References


[1] Theoretical Principles of Electrotechnics. Moscow: High School, 2 (1976), p.137-174, 182-184, 218-225.

[2] Korablev V.M., Tkachenko L.M. Preprint IHEP 95-44. NIM Section A, Reg.No: BAR–95:110

[3] Bencze Gy.L. et al. Study of resistive plate chambers for muon detection at hadron colliders. NIM A340 (1994), p.466–473.



*Received July 2, 1996*


## Appendix

Here we present the analytical expressions of the integrals for electric field calculation from the surface charge density $\sigma$ in the intrinsic frame of reference, where z–coordinate is the normal to surface element.

If we direct radius vector $\vec{r}$ from the given space point to the surface element ds=dx·dy, the electric field in this point can be expressed as:

$$E_x = -\sigma \cdot k \int_s \frac{x}{r^3} ds = \sigma \cdot k \cdot ln|y + r| = \sigma \cdot G_x, \tag{20}$$

$$E_y = -\sigma \cdot k \int_s \frac{y}{r^3} ds = \sigma \cdot k \cdot ln|x + r| = \sigma \cdot G_y, \tag{21}$$

$$E_z = -\sigma \cdot k \int_s \frac{z}{r^3} ds = -\sigma \cdot k \cdot \frac{z}{|z|} \frac{x}{|x|} arctg \frac{y|x|}{|z|r} = \sigma \cdot G_z, \tag{22}$$

$$U = \sigma \cdot k \int_s \frac{ds}{r} = \sigma \cdot k \cdot (x \cdot ln|y+r| + y \cdot ln|x+r| - |z| \cdot \frac{x}{|x|} arctg \frac{y|x|}{|z|r}) \qquad (23)$$

here k=1/4$\pi$.

If the space point is placed in the centre of the surface element, then the own integrals (from square of the given element) for tangential field components (20) and (21) are equal to zero.

Now about the calculation of tangential field derivative $dE_t/dt$.

Let $\vec{t} = \{dx/dt, dy/dt, dz/dt\} = \{\alpha, \beta, \gamma\}$ denote the unit vector along $E_t$ direction, then:

$$\begin{aligned} \frac{dE_t}{dt} &= \alpha(\alpha\frac{\partial E_x}{\partial x} + \beta\frac{\partial E_x}{\partial y} + \gamma\frac{\partial E_x}{\partial z}) + \beta(\alpha\frac{\partial E_y}{\partial x} + \beta\frac{\partial E_y}{\partial y} + \gamma\frac{\partial E_y}{\partial z}) + \\ &+\gamma(\alpha\frac{\partial E_z}{\partial x} + \beta\frac{\partial E_z}{\partial y} + \gamma\frac{\partial E_z}{\partial z}) \end{aligned} \qquad (24)$$

and, as is easy to check:

$$\frac{\partial E_x}{\partial y} = \frac{\partial E_y}{\partial x}, \quad \frac{\partial E_x}{\partial z} = \frac{\partial E_z}{\partial x}, \quad \frac{\partial E_y}{\partial z} = \frac{\partial E_z}{\partial y}. \qquad (25)$$

The analytical expressions for integrals from partial derivatives:

$$\int_s \frac{\partial E_x}{\partial x} ds = -\sigma \cdot k \frac{xy}{(x^2+z^2)r}, \qquad (26)$$

$$\int_s \frac{\partial E_y}{\partial y} ds = -\sigma \cdot k \frac{xy}{(y^2+z^2)r}, \qquad (27)$$

$$\int_s \frac{\partial E_z}{\partial z} ds = \sigma \cdot k \frac{xy(z^2+r^2)}{(x^2y^2+z^2r^2)r}, \qquad (28)$$

$$\int_s \frac{\partial E_x}{\partial y} ds = \sigma \cdot k \frac{1}{r}, \qquad (29)$$

$$\int_s \frac{\partial E_x}{\partial z} ds = \sigma \cdot k \frac{z}{(y+r)r}, \qquad (30)$$

$$\int_s \frac{\partial E_y}{\partial z} ds = \sigma \cdot k \frac{z}{(x+r)r} \qquad (31)$$

and tangential field derivative $dE_t/dt$ for the given element can be presented as the linear combination of surface charge densities $\sigma$, in which coefficients near unknowns $\sigma$ are the numerical values of integrals.

В.Аммосов, В.Кораблев, В.Заец.
Электрическое поле и токи в резистивной плоскопараллельной камере.

Оригинал-макет подготовлен с помощью системы LaTeX.
Редактор Е.Н.Горина. Технический редактор Н.В.Орлова.

Подписано к печати 05.07.96. Формат 60 × 84/8. Офсетная печать.
Печ.л. 2.25. Уч.-изд.л. 1.72. Тираж 240. Заказ 725. Индекс 3649.
ЛР №020498 06.04.92.

ГНЦ РФ Институт физики высоких энергий
142284, Протвино Московской обл.

Индекс 3649

П Р Е П Р И Н Т 96-52, И Ф В Э, 1996